

# A PLANAR MOTOR WITH ELECTRO-DYNAMIC PROPULSION AND LEVITATION UNDER 6-DOF CONTROL

**J.C. Compter**

Philips, Centre for Industrial Technology  
P.O.box 218/ SAQ 1406, 5600 MD, Eindhoven, The Netherlands  
Tel: +31 40 2732902 Fax: +31 40 2733201  
Email: J.C.Compter@philips.com

**Abstract**—An electronically commutated planar motor based on Lorentz forces is described as a potential drive in the highly demanding applications of the semiconductor industry. An extended Halbach array forms the basis of the design. Four three-phase forcers are capable of delivering the required forces to control the planar motor over the six degrees of freedom. The position information required for the electronic commutation is obtained by a number of Hall sensor arrays. The positive results of the prototype testing encourage further use in industrial applications under vacuum conditions.

**Key words**—planar, Lorentz, levitation, Halbach.

## 1. INTRODUCTION

The classic method of obtaining a long stroke XY movement is to use a gantry together with two or more linear motors. The use of a gantry in high vacuum conditions, however can cause problems from contamination by the grease of the roller bearings. Air bearings are an alternative, but their weight and size limits the system performance. As a solution, the use of a planar motor based on Lorentz forces is proposed. Magnetic forces are employed to control the movement of the motor over the six degrees of freedom (6-DoF).

The design is based on an extended Halbach array [1]. Four three-phase forcers, each consisting of three air coils, and a number of Hall sensor arrays produce the actual X and Y position as input for the electronic commutation. Each forcer is capable of producing both a levitating force and a force in the horizontal XY plane. Two forcers are used in the X-direction, and two in the Y-direction.

Details of several planar motor designs have been published. D. Trumper [2] developed levitation linear motors for use with lithography systems. Electro-magnetically driven long XY-stroke platforms based on the Sawyer linear stepper motor with mechanical bearings are described by A.E. Quaid [3]. W. Kim [4] describes a levitated platform with a short stroke. Flores Filho [5] analysed a long stroke planar motor with a moving magnet and mechanical bearings. Electro-dynamically levitated and propelled platforms are described by H. Chu, [6], J. Hazelton [7] and S. Jung [8].

Our concept is based on a moving coil designed for a long XY-stroke with levitation and a stable servo performance. Section 2 describes the concept of the planar motor, Section 3 the Halbach array and Section 4 describes the forcers and the interaction between the array and the forcers. Section 5 deals with the Hall sensor arrays.

## 2. THE CONCEPT

### 2.1. Moving coils or magnets

Initially, a planar motor based on moving magnets seems to be the ideal solution, because moving motor cables are not needed, and the heat generated in the coils can easily be removed. However, coils should cover the full operating area of the motor. To reduce the costs of the amplifiers and heat removing components, one might only activate the coils in the region of the magnets, but then an extended array of switching power electronics is needed to control the individual coils. It was considered that this would have an impact on the mean time between failures. Because of this, we decided to use moving coils and to work on solutions for the moving power cables and the heat removal from the moving parts.

### 2.2. The magnets and forces in the X-, Y- and Z-direction

A Halbach magnet array, as shown in Fig. 1, creates a field with X- and Z-components. A current carrying conductor will experience X- and Z-forces in a ratio depending on its x-position. This means that X- and Z-forces can be readily generated, but forces in the Y-direction, however, have to be generated by a planar motor.

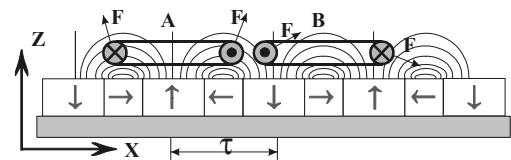


Figure 1. Halbach array on an iron yoke and a coil

The first step is to extend the magnet array to a two-dimensional one, as shown in Fig. 2.

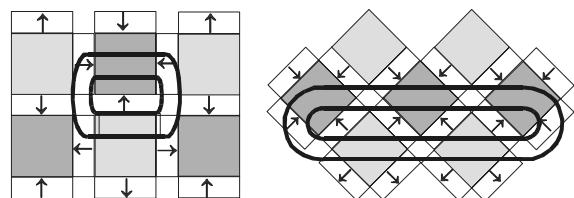


Figure 2. The extended Halbach array with potential coils

A short coil will generate horizontal and vertical forces, but its length should not exceed the dimensions of the square magnets to prevent loss of force. This would suggest the use of many small coils, leading to rising costs. The solution we propose is to rotate the magnets 45 degrees with respect to the

coils. A coil, perpendicular with respect to the one shown, will produce X-forces. The proposed design is based on separate coils sets, called forcers, for the X-Z- and the Y-Z-directions. Fig. 3 shows a single Y-forcer with a width of  $4\tau$  and the orientation of the four forcers required to produce X, Y and Z forces and torques.

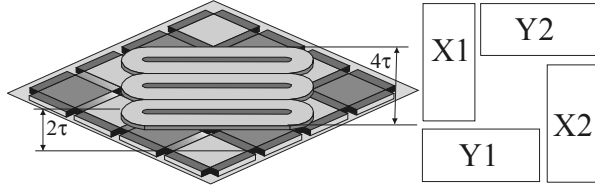


Figure 3. A Y-forcer above an extended Halbach array with iron yoke and the orientation of all four forcers.

### 3. THE HALBACH MAGNET ARRAY

The Halbach array used consists of magnets with their magnetisation perpendicular and parallel to an iron yoke. A 3-dimensional Finite Element Modelling is used initially to obtain the field values, but because of long processing time we decided to use a model based on the field equations given by [9] for a single magnet in free air for the final optimisation of the geometry. The field components for a magnet with  $B_r$  as remanence, magnetised in the Z-direction and  $\mu=\mu_0$  are at a point  $x,y,z$  in the coordinates of Fig. 4, are:

$$B_c = \frac{B_r}{4\pi} \sum_{i=0}^1 \sum_{j=0}^1 \sum_{k=0}^1 (-1)^{i+j+k} \epsilon_c(S,T,R) \quad (1)$$

With c referring to  $x, y$  or  $z$  and:

$$\epsilon_x = \ln(R-T), \quad \epsilon_y = \ln(R-S), \quad \epsilon_z = a \tan\left(\frac{ST}{RU}\right), \quad (2-3)$$

$$S = x - a(-1)^i, \quad T = y - b(-1)^j, \quad U = z - h(-1)^k, \quad (4-6)$$

$$R = \sqrt{S^2 + T^2 + U^2}. \quad (7)$$

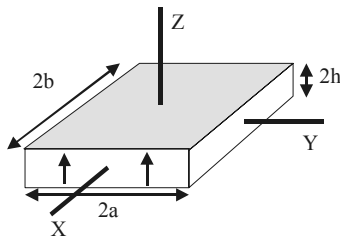


Figure 4. A magnet in free air

The first step in translating a full Halbach magnet array on an iron yoke is to mirror the magnets in the iron yoke (see Fig. 5) according to [10].

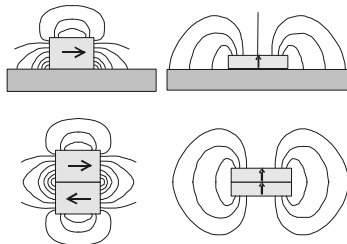


Figure 5. Magnet mirroring

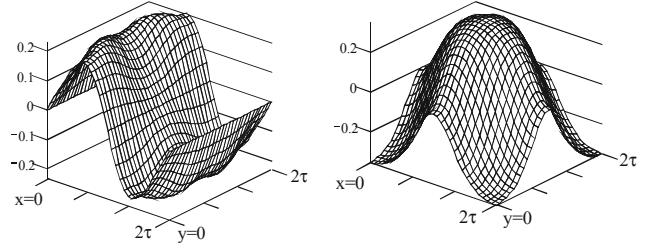


Figure 6. The field strength  $B_x$  and  $B_z$  above the magnets in Tesla

## 4. THE COILS

### 4.1. The enclosed flux and forces

It is the intention to apply the principle of AC-synchronous brushless motors, so that the enclosed fluxes  $\psi_{ph}$  and currents  $i_{ph}$  in the coils behave sinusoidally as a function of the position  $x$ . Let us assume that the enclosed fluxes of the coils  $ph=1-3$  of an X-forcer behave as:

$$\Psi_{ph}(x,z) = \hat{\Psi}_0 e^{-\alpha z} \sin(\pi x / \tau + \varphi + (ph-1)4\pi/3) \quad (8)$$

With:

$x$  relative position

$z$  distance coil to magnets

$\hat{\Psi}_0$  enclosed flux at  $z=0$

$\alpha$  magnet geometry related constant

$\varphi$  phase shift of the field with respect to the  $x$ -coordinate.

An implicit assumption here is that a coil pitch of  $4/3\tau$  is applied.

The currents  $i_{ph}$  should behave as:

$$i_{ph}(x) = \hat{I} \sin(\pi x / \tau + \varphi + (ph-1)4\pi/3 + \theta) \quad (9)$$

Here  $\hat{I}$  is the current amplitude and  $\theta$  an additional phase angle, which determines the force direction as will be shown. For permanent magnet-based 3-phase actuators the forces  $F_x$  and  $F_z$  are given by:

$$F_x = \sum_{ph=1}^3 i_{ph} \frac{\partial \Psi_{ph}}{\partial x} = \frac{3\pi}{2\tau} \hat{I} \hat{\Psi}_0 e^{-\alpha z} \cos(\theta) = K_x \hat{I} \cos(\theta) \quad (10)$$

$$F_z = \sum_{ph=1}^3 i_{ph} \frac{\partial \Psi_{ph}}{\partial z} = -\frac{3}{2} \alpha \hat{I} \hat{\Psi}_0 e^{-\alpha z} \sin(\theta) = K_z \hat{I} \sin(\theta) \quad (11)$$

Therefore the phase angle  $\theta$  determines the ratio between the force components and the length of the force vector is expressed by  $\hat{I}$ . As is usual for AC-synchronous brushless motors, the assumed currents remove the position dependency of the forces. So the design target for the coil and magnet geometry is to produce the assumed flux function at the nominal value of the position  $z$ . This minimum value is based on a realistic flatness of the Halbach array and underside of the forcers.

### 4.2. Coil design

When considering the coil design we should take into account the required sinusoidal behaviour of the flux as a function of position, as mentioned in the previous section. The motion profile to be produced gives rise to other design aspects:

- the loss  $P$  should remain acceptable, so consider:

$$\frac{F_{rms}^2}{P} \propto \frac{(m_{load} + m_{coils})^2}{P} \quad (12)$$

with:

- $F_{rms}$  effective force (levitation *and* acceleration),
- $P$  the losses in all forcers,
- $m_{load}$  the payload,
- $m_{coils}$  the mass of the coils.

- the required voltage, peak and rms current of the 3-phase power supply
- the temperature rise of the coils and the heat flow to the environment.

Critical design factors are the length  $l_{coil}$  and height  $h_{coil}$  of the coils, the choice of the conductor material (aluminium or copper), the form of the conductors (round or square wire or foil), the number of turns and the method of heat removal. When examining simulations of potential coil heights, we found at a fixed value of the height  $z$ , a minimized position dependency of the motor force at a certain coil height  $h_{coil}$ , giving also  $K_x=K_y=K_z$ . Clearly this is the point where a sinusoidal behaviour of the flux is obtained, as indicated in Section 4.1. So there exists a link between the losses  $P$ , the value of  $z$ ,  $h_{coil}$  and a minimum position dependency of the force.

In Section 4.1 we assumed that the flux  $\psi_{ph}$  does not depend on the  $y$ -position; this is obtained by tuning the length of the coil,  $l_{coil}$ . The final result is, that one can only extend  $l_{coil}$  in steps of  $2\tau$ .

To determine the optimum width of the inner space of the coils we used (12) as a reference.

Until now our attention was directed at the force component in the X,Y and Z-direction, however unwanted torques over the X,Y and Z-axis can also exist. Following the procedure given we noticed that a  $y$ -torque  $T_y$  remains present at all times. Its value can be determined with the model shown in Fig. 7.

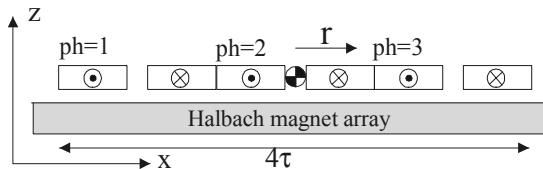


Figure 7. Model to predict the pitch torque  $T_y$

With the phase currents according to (9) and  $B_y$  and  $B_z$  behaving as a sine and a cosine and  $z$ -independent, we find pitch torque  $T_y$  as:

$$T_y = \frac{4\tau}{3\sqrt{3}} \left\{ F_x \sin\left(\frac{2\pi x}{\tau}\right) + \frac{F_z K_x}{K_z} \cos\left(\frac{2\pi x}{\tau}\right) \right\} + f(F_x, F_z) \quad (13)$$

This relationship is confirmed by FEM modelling and experiment. Notice  $\tau$  as the only free design parameter. The last term of (13) is more than one order smaller than the first one and will be ignored.

The remaining torque can be compensated for by the second  $x$ -forcer giving the same torque with opposite polarity by shifting the forcers over  $(n+0.5)\tau$  with respect to one another ( $n$ : integer). This is only valid, however, when both forcers are producing the same force components  $F_x$  and  $F_z$ . This last condition cannot be fulfilled during accelerations, so there

always remains a torque to be counteracted by the servo control-loop, e.g. by feed-forward.

### 4.3. Design tool

Section 3 describes the modelling of the Halbach array and Section 4.2 a number of constraints and design targets. In the magnet array, one can find four independent magnet dimensions. The same number applies to the coils. The relative position of the magnets to the coils can be expressed by the independent variables  $x$ ,  $y$  and  $z$ . To investigate the relationship between all parameters, a Mathcad™ model is built based on (1) to (7), in combination with the well-known Lorentz force and torque equations:

$$\vec{F}(x, y, z) = \sum_{phase=1}^3 \iiint_{V_{phase}} \vec{I} \times \vec{B} dV \quad (14)$$

$$\vec{T}(x, y, z) = \sum_{phase=1}^3 \iiint_{V_{phase}} \vec{r} \times \vec{I} \times \vec{B} dV \quad (15)$$

This Mathcad™ model, running on a 1 GHz processor, can predict within ten minutes the forcer performance of 900  $(x,y,z)$  positions. This gives a fast and comprehensive overview of geometrical changes.

The model predicts that by careful design the position dependent variations in the force components can be reduced to less than 1 % of the force amplitude. This means that mechanical tolerances, magnet strength variations and amplifier errors will be the major cause of motor-related control loop disturbances.

According to (13) one can expect a pitch torque amplitude of 3.74 Nm at  $\tau=32$  mm and  $F_x=152$  N. Fig. 8 shows the behaviour of this torque  $T_y(x,y)$  as predicted by the Mathcad-model, giving 3.79 Nm as amplitude. The amplitude of the other torque components  $T_x$  and  $T_z$  is one order lower.

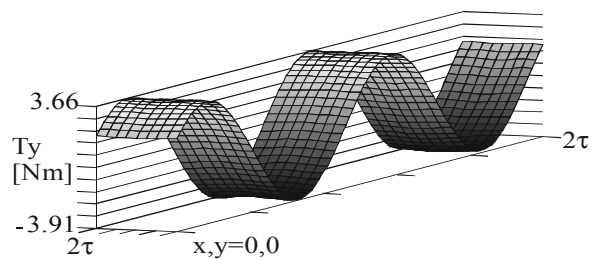


Figure 8. Pitch torque at  $F_x=152$  N,  $F_z=0$  N and  $\tau=0.032$  m

Fig. 9 shows the predicted behaviour of the force  $F_x(x,y)$  which is in general well suited to servo applications. The conclusion is that a planar motor is defined with a promising servo-behaviour and simple coil geometry. To control the planar motor one needs four 3-phase power amplifiers.

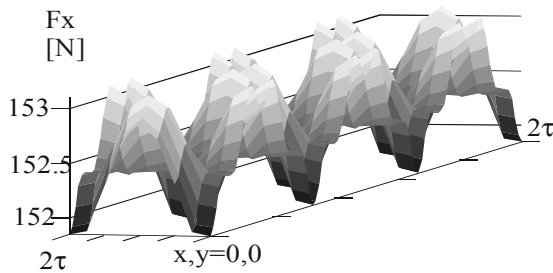


Figure 9. Force  $F_x$  at  $F_z=0$  N

## 5. HALL ARRAY SENSOR

The relationship between currents in this AC-synchronous brushless motor and the physical position  $x$  is given by (9). The absolute position with respect to the magnet plate is the angle  $\varphi$  in (9). During the experiments we used Hall sensor arrays as shown in Fig. 10.

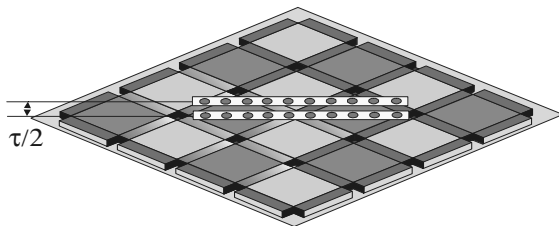


Figure 10. Hall sensor arrays

Each array consists of  $n$  Hall sensors at a distance  $n/(n+1) \cdot 2\tau$ . Summing the Hall sensor signals gives an  $y$ -dependent sine function, which is nearly  $x$ -position independent. With two arrays at a distance  $\tau/2$  one obtains the usual S0/S90 signals, which enable a position measurement within a range of  $2\tau$ . A second set of Hall arrays, directed in the same direction, allows the measurement of the rotation over the  $z$ -axis, and a third set, perpendicular to the previous sets, enables an  $x$ -position measurement. The amplitude of the sensors contains information related to the  $z$ -position, although we used inductive sensors for the  $z$ -position.

The test set-up showed an X-Y-position accuracy of  $0.005\tau$ , which is sufficient for the control of the motor currents. Another sensor system is required when a greater accuracy is needed for control purposes, e.g. a laser interferometer or an incremental X-Y optical sensor.

## 6. STATUS

Tests confirm the results described in this paper. Identified sources of errors are gain errors and offsets in the power amplifier and Hall sensors.

In the first instance, the control per degree of freedom was developed separately with the remaining degrees of freedom fixed by mechanical means. The experience gained and the knowledge we now have means that a full 6-DoF controlled planar motor can be manufactured. Several patents have been filed [11]-[14] and further information relating to the control and amplifier requirements will be available in the future.

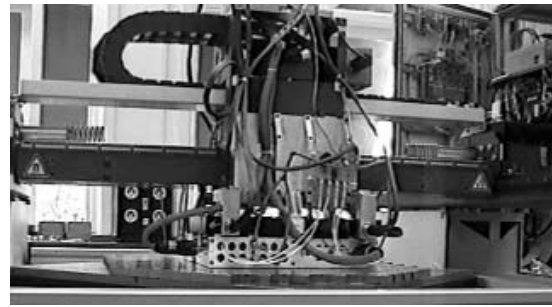


Figure 11. Test setup

## 7. CONCLUSION

A new planar motor geometry based on an extended Halbach array and Lorentz forces is described and its modelling and design tools analysed. This planar motor requires electronic commutation, and the necessary positional information is obtained by Hall sensor arrays sensing the field of the Halbach array.

## REFERENCES

- [1] K. Halbach, "Design of Permanent Multipole Magnets with Oriented Rare Earth Cobalt Material" Nuclear Instruments and Methods, 169, 1980, pp. 1-10.
- [2] D.L. Trumper, "Magnetic Suspension Techniques for Precision Motion Control", Ph.D., Electrical Engineering, MIT, September 1990
- [3] A.E. Quaid, A.A. Rizzi, "Robust and efficient Motion Planning for a planar Robot using Hybrid Control" IEEE Int. Conf. On Robotics & Automation, San Francisco, April 2000, pp. 4021-4026.
- [4] W. Kim, D.L. Trumper, J.H.Lang., "Modeling and vector control of a planar magnetic levitator". IEEE Industry Application Soc., 32nd Annual Meeting, October. 1997, pp. 1-8
- [5] A.F. Flores Filho, A.A. Susin, M.A. da Silveira, "Development of a new Electromagnetic planar actuator" Preprints of the 1st IFAC-conference on Mechatronic Systems, Vol. 1, Sept. 2000, pp. 359-364
- [6] H. Chu, H. Jung, "Effect of coil position and width on back EMF constant of permanent magnet planar motors" Int. Electric Machines & Drives Conf. 2000, pp. 430-435
- [7] A.J. Hazelton, J.M. Gery, Patent US 6,285,097 B1, Planar electric motor and positioning device having transverse magnets
- [8] K.S. Jung, Y.S. Baek, "Study on a novel Contact-Free Planar System Using Direct Drive DC Coils and Permanent Magnets" IEEE/ASME Trans. On Mechatronics, Vol 7, No 2, March 2002
- [9] G. Akoun, J. Yonnet, "3D analytical calculation of the forces exerted between two cuboidal magnets" IEEE Trans. on Magnetics, Vol 20, No 5, September 1984, pp. 1962-1964
- [10] K. Binns, P.J. Lawrenson, C.W. Trowbridge, Electric and magnetic fields, John Wiley & Sons, ISBN0-471-92460-1, 1992, pg. 24
- [11] P. Frissen, et al, "Displacement device", US 6531793
- [12] J. Compter, P. Frissen, "Displacement device", US 6496093
- [13] P. Frissen, et al, "Displacement device", US 2002/0079888
- [14] J. Compter, "Displacement device", US 2002/0000904